Intrinsic defects in GaN. I. Ga sublattice defects observed by optical detection of electron paramagnetic resonance

K. H. Chow,* L. S. Vlasenko,† P. Johannesen,‡ C. Bozdog,§ and G. D. Watkins
Department of Physics, Lehigh University, 16 Memorial Drive East, Bethlehem, Pennsylvania 18015-3182, USA

Akira Usui,¶ Haruo Sunakawa,¶ Chiaki Sasaoka, and Masashi Mizuta
Photonic and Wireless Devices Research Laboratories, NEC Corporation, Seiran 2-9-1, Ohtsu, Shiga 520-0833, Japan
(Received 10 September 2003; published 29 January 2004; publisher error corrected 4 February 2004)

Irradiation of GaN by 2.5-MeV electrons *in situ* at 4.2 K produces a broad photoluminescence (PL) band centered at 0.95 eV. Optical detection of electron paramagnetic resonance (ODEPR) in the band reveals two very similar, but distinct, signals, L5 and L6, which we identify as interstitial Ga^{2+} in two different lattice configurations. L5, present immediately after the irradiation, is seen via a spin-dependent electron transfer process from the shallow effective-mass donor (EM) which competes with the PL (negative signal). L6 emerges upon annealing at various stages starting at ~60 K, possibly assisted by optical excitation, as a spin-feeding process (positive signal) not involving the EM donor. Both L5 and L6 disappear upon prolonged annealing at room temperature, with L6 disappearing first. Most of the 0.95-eV band (~85%) also disappears in this anneal, the remaining fraction being stable to ~500 °C. Two tentative models are presented, each of which identifies L5 and L6 with Ga^{2+} in different interstitial sites near the gallium vacancy from which they were created. Both models ascribe the 0.95-eV PL band, along with an ODEPR signal observed in it L1 as arising from the Ga vacancy, which in its isolated form is therefore stable to ~500 °C.

DOI: 10.1103/PhysRevB.69.045207 PACS number(s): 71.55.Eq, 61.72.Ji, 61.82.Fk, 76.70.Hb

I. INTRODUCTION

Vital to the successful optical or electronic application of any semiconductor is the understanding of its intrinsic defects, i.e., lattice vacancies and interstitials, because they provide the various diffusion mechanisms involved in processing and device degradation, as well as in often controlling background doping, compensation, minority-carrier lifetime, and luminescence efficiency. Currently there is much interest in the wide-bandgap semiconductor gallium nitride (GaN) because of its proven success for light emitting and laser applications, and its potential for high-temperature electronic applications.[1] Although there have been several theoretical studies of vacancies and interstitials in GaN,[2–7] little experimental information presently exists. The only direct and unambiguous method of introducing these defects for experimental study is by high-energy electron irradiation, where host atoms can be displaced from their lattice sites by Rutherford scattering. In addition, the most successful experimental technique for identifying and studying the defects has proven to be electron paramagnetic resonance, detected either directly (EPR) or optically (ODEPR). Studies combining room temperature electron irradiation and ODEPR have recently been reported,[8,9] leading to the observation of several new defects produced by the irradiation, labeled L1–L4, two of which (L3 and L4) were tentatively identified as trapped Ga interstitials.[9] This observation strongly suggested that the Ga interstitial must be mobile below room temperature.

Here we describe a continuation of these studies, where the electron irradiation has been performed *in situ* at 4.2 K, to freeze in the primary defects for study before their movement is possible. An early result of the experiments has already been published, where an isolated Ga interstitial was identified.[10] These studies have been continued and in the present paper we describe in detail what has been learned. We find that interstitial Ga can actually be observed in two distinctly different configurations. We will propose two possible models for them, each of which identifies them to be in different lattice sites near the gallium vacancy from which they were ejected. In addition, we will supply evidence that one of the defects previously detected in the room-temperature irradiations (L1) may be the isolated Ga vacancy.

In a companion paper immediately following this one,[11] hereafter to be referred to as B, the mechanism for conversion between the two interstitial configurations will be explored.

II. EXPERIMENTAL DETAILS

Most of the samples studied were free standing, thick (200–500 μm), single wurtzite crystal platelets of GaN grown at NEC by hydride vapor phase epitaxy (HVPE) using a facet-initiated epitaxial layer overgrowth (FIELO) technique on a GaN-nucleated *c*-axis sapphire substrate which was subsequently removed. The details are described in Ref. 12. The samples were not intentionally doped, being *n* type, with $n<10^{17}$ cm^{-3}, and with very low dislocation content ($\sim 10^7$ cm^{-2}). Samples from three such platelets, grown at different times, labeled VPE2-155, VPE2-180, and VPE2-331 were studied. In addition, a 3-μm thick *p*-type sample grown by metal-organic vapor phase epitaxy (MOVPE) on *c*-axis sapphire, labeled MOVPE-208B, was also studied.

The experimental setup used to obtain the data described in this paper is identical to that of earlier ODEPR work on II-VI semiconductors, which should be referred to for further details.[13] Briefly, the experiments were performed at 20 GHz in an EPR spectrometer capable of irradiation *in situ* at 4.2 K with 2.5-MeV electrons from a Van de Graaff accelerator.

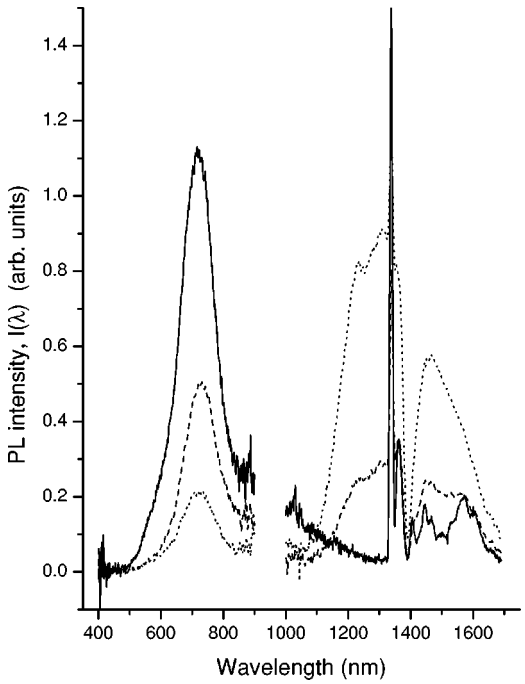

FIG. 1. PL spectra, corrected for monochromator and detector spectral response, for sample VPE2-155c at 1.7 K before and after 2.5-MeV electron irradiation *in situ* at 4.2 K. Solid: before irradiation; dashed: after $0.6\times10^{17}e/\mathrm{cm}^2$; dotted: after $1.3\times10^{17}e/\mathrm{cm}^2$. (The dip at ~1400 nm is an artifact resulting from absorption in the quartz light pipe used to extract the PL from the cryostat.)

Subsequent ODEPR experiments were accomplished by inserting into the TE_{011} microwave cavity a fused quartz capillary tube, which served as a light pipe to extract the photoluminescence (PL), and within which was threaded an optical fiber which allowed for the sample (located a few millimeters below the lightpipe) to be photoexcited with ultraviolet light. To monitor the ODEPR signals, the luminescence was detected with either a silicon (EG&G 250UV) or cooled germanium (North Coast EO-817S) diode detector, and, for most of the experiments, excitation ($\leqslant$3 mW) was supplied by the 364-nm (3.41-eV) line of an argon-ion laser. This wavelength is just below the low-temperature bandgap of GaN (3.51 eV) and allowed for bulk penetration of the thick samples, which were immersed in pumped liquid helium (~1.7 K). Microwave power from a 300-mW Gunn diode was on-off modulated at ~200 Hz, and synchronous changes in the luminescence were detected via lock-in detection. The platelet sample was indium soldered onto a brass post, cut at 45° in order to provide equal surface area for the horizontal electron irradiation and subsequent vertical photoexcitation. (The magnetic field could be rotated in the horizontal plane and therefore only directions between $\mathbf{B}\perp c$ axis and 45° to the *c* axis were accessible.)

III. RESULTS

In Fig. 1 we show the characteristic photoluminescence observed in one of the *n*-type HVPE samples before and after irradiation *in situ* at 4.2 K.

This behavior was similar in all of our *n*-type samples.

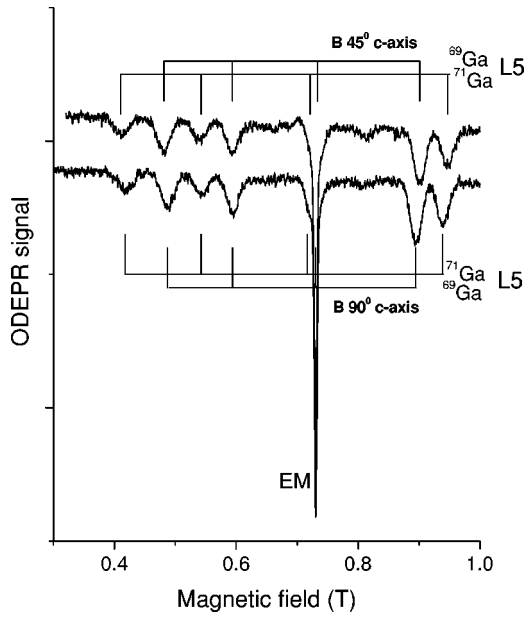

FIG. 2. ODEPR spectrum observed in the 0.95-eV PL band at 1.7 K for sample VPE2-180b after $5\times10^{16}e/\mathrm{cm}^2$ *in situ* irradiation at 4.2 K.

Before irradiation, the visible luminescence is dominated primarily by a broadband at ~700 nm, which appears to be the characteristic of low-dislocation samples grown by the HVPE method.[14,15] This band decreases in intensity monotonically with irradiation dose. In the infrared, a strong zero-phonon line (ZPL) at ~1350 nm and associated phonon structure is initially present, again characteristic of all of our HVPE samples, which has been attributed to vanadium (V^{3+}).[16] Its intensity also decreases with irradiation as a strong broadband centered at ~1300 nm (~0.95 eV) grows in. Within our accuracy, this band is identical to that previously observed to result from room-temperature irradiation,[8,9] but its production rate is substantially greater ($\sim\times5$).

The ODEPR spectrum observed in the 0.95-eV band immediately after the 4.2 K irradiation is shown in Fig. 2. None of the signals seen previously in this band after the room-temperature irradiations[8,9] are present. Instead, two negative signals are seen, one single line associated with the shallow effective-mass (EM) donor,[17] as indicated, the other a set of lines which we have labeled L5. The positions of the L5 lines can be accurately fit by the following spin Hamiltonian:

$$\mathcal{H}=\mu_B\mathbf{S}\cdot\mathbf{g}\cdot\mathbf{B}+\mathbf{S}\cdot\mathbf{A}\cdot\mathbf{I}-g_n\mu_N\mathbf{I}\cdot\mathbf{B}, \quad (1)$$

where **B** is the external magnetic field, μ_B denotes the Bohr magneton, μ_N represents the nuclear magneton, and **A** is a hyperfine tensor which couples the electronic spin **S** to a nuclear spin **I** for which the nuclear *g* value is g_n. As shown in Fig. 2, the structure is accurately reproduced by assuming that L5 is an $S=1/2$ center with a strong, slightly anisotropic, hyperfine interaction from a single Ga nucleus (isotopic abundance: 60% ^{69}Ga, 40% ^{71}Ga; $g_n^{69}/g_n^{71}=0.787\,03$, and for both, $I=3/2$). The spin-Hamiltonian parameters are given in Table I, where ''parallel'' refers to the *c* axis of the

TABLE I. Spin-Hamiltonian parameters for the ODEPR signals.

Signal	$g_\perp$	$g_\parallel$	$^{69}A_\perp$(GHz)	$^{69}A_\parallel$(GHz)
L5	2.000(1)	2.000(3)	3.77(1)	4.01(3)
L6	1.999(2)	1.999(4)	3.85(2)	4.05(4)
L6*	2.000(3)	2.000(5)	3.84(2)	4.00(5)
L1	2.008(1) [a]	2.004(1) [a]	0.10(1)	0.10(1)

[a]Reference 9.

wurtzite crystal. In some of the samples studied, the two signals could also be observed weakly, again negative, in the visible luminescence.

Figure 3 shows the result of an isochronal (30 min) annealing sequence for the ODEPR signals in the sample of Fig. 2. At each temperature, a 30-min anneal was first performed in the dark followed by a 30-min anneal with the laser on. There are several interesting effects occurring, which we now consider: (i) L5 and the negative EM signal remain present up to the 295 K anneal, at which point they disappear together. Continued annealing at this temperature, shown in the inset, reveals a time constant for the disappearance of L5 (and EM) of $\sim$200 min.[10] Simultaneous with their disappearance, L2 grows in and there is a corresponding growth in of L1, both L1 and L2 being signals previously studied, but not identified, in room-temperature irradiated GaN.[8,9] (ii) A different signal, labeled L6, emerges at various stages throughout the lower-temperature annealing sequences. In this particular sample (VPE2-180b), its intensity was very weak, and it was initially missed.[10] Figure 4(b), however, shows the spectrum in a different and more heavily irradiated sample (VPE2-331c) after 200 K anneal and prolonged laser illumination, where, because of the stronger

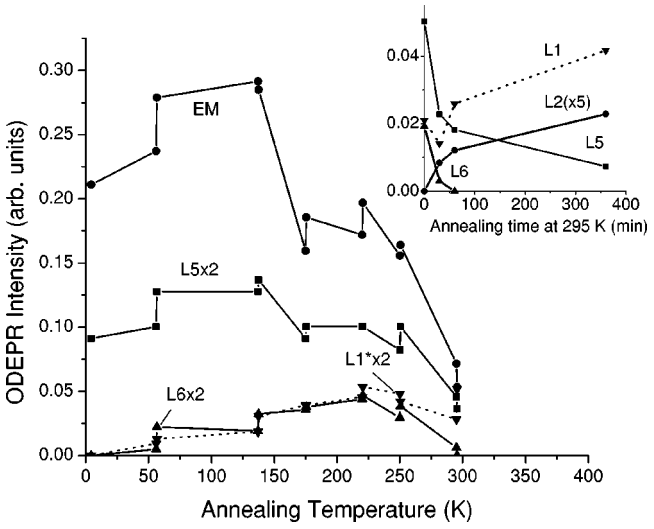

FIG. 3. Result of isochronal annealing on the amplitudes of the various ODEPR spectra observed in the 0.95-eV PL band for the VPE2-180b sample of Fig. 2. At each temperature the sample was annealed first for 30 min in the dark and then 30 min under laser excitation. (Plotted for L5 and L6 are the amplitudes of their high-field ^{69}Ga line.) The recovery vs annealing time at 295 K is shown in the inset.

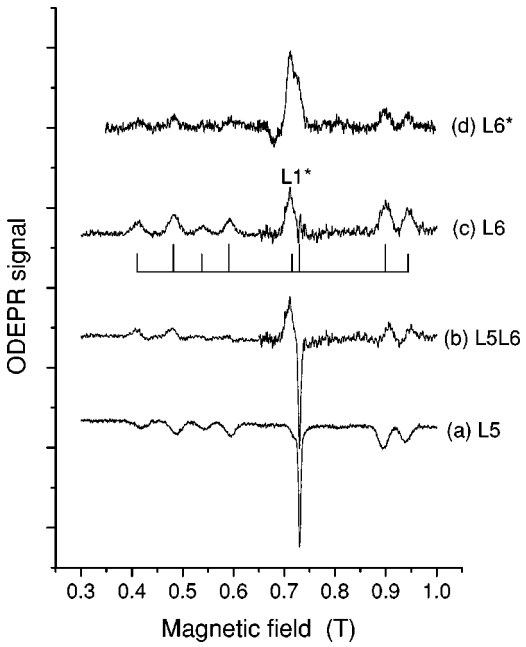

FIG. 4. (b) ODEPR spectrum, $\mathbf{B}\perp\mathbf{c}$, in sample VPE2-331c after $1.6\times10^{17}e/\mathrm{cm}^2$ at 4.2 K, subsequent anneal at 200 K, and several days of study under optical excitation at 1.7 K. (c) Signal L6 plus L1*, after subtracting from (b) the component of L5 shown in (a). The sticks show the positions for the L6 lines predicted by the spin-Hamiltonian parameters in Table I. (d) The L6* signal observed in the *p*-type MOVPE sample after 260 K anneal.

relative intensity of L6, it was possible to separately extract it, as shown in Fig. 4(c), and estimate its spin-Hamiltonian parameters. These parameters are included also in Table I. (The greater uncertainty indicated for the L6 parameters than for those of L5 reflects an estimate of the additional possible error in this nontrivial extraction.) Once identified in this fashion, it was possible to go back to the spectra for the Fig. 3 annealing sequence and extract the L6 contribution at each stage, as shown. (The detailed method for this extraction is described in B.) L6 is a *positive* signal, which like the *negative* L5 signal, displays hyperfine interaction with a single Ga atom, and which is only a few percent larger than that for L5. No EM signal appears to be associated with it. L6 is less stable than L5, annealing faster at 295 K. (iii) Another positive signal which appears to be indistinguishable from L1,[9] but which we tentatively label L1*, begins to grow in at the lower-temperature anneal stages roughly in synchronism with the growth in of L6. It is more apparent in Fig. 4(c), as indicated, where the strength of L6 is greater. (iv) There is a strong suggestion that illumination speeds up the annealing process in the lower-temperature stages. Spectral dependence studies reveal both L5 and L6 to accurately mirror the 0.95-eV band.

Figure 5 shows the result of annealing on the various PL bands for the sample VPE2-180b of Fig. 2. There is evidence of partial recovery at various low-temperature stages, as seen also for the ODEPR in Fig. 3, but, as for the ODEPR, the major change occurs at the 295 K anneal, with the loss of most of the 0.95-eV band. At that point, the characteristic 0.88-eV PL band[9] of L2 is observed to emerge, mirroring

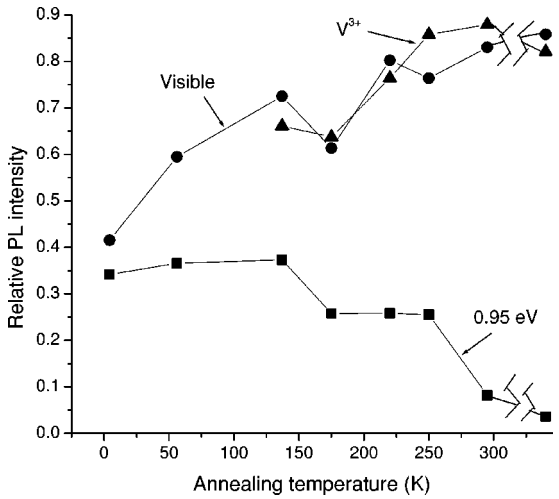

FIG. 5. Intensities of the PL bands after the total 60-min annealing time at each temperature for sample VPE2-180b, as shown for its ODEPR spectra in Fig. 3. Shown also after the broken lines are the values after several days at room temperature. The points for the visible and V^{3+} PL have been normalized to their values before irradiation. The normalization for the 0.95-eV PL is arbitrary.

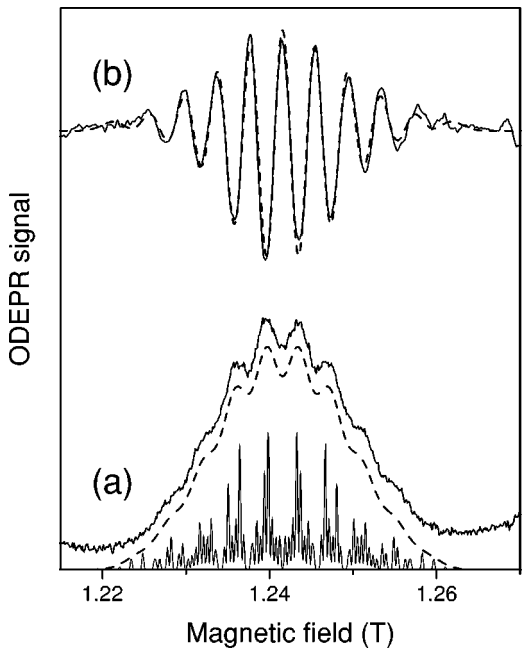

FIG. 6. (a) ODEPR spectrum at 35 GHz of L1, and (b) its second derivative, for $\mathbf{B}\perp\mathbf{c}$, compared to predictions for hyperfine interactions with three equivalent Ga atoms, as shown by the sticks, and, after convoluting with a Gaussian of appropriate width, by the dashed curves.

that observed in the ODEPR. The remaining 0.95-eV band ($\sim$10–15% of its original intensity) has previously been shown to be stable to $\sim$500 °C.[9]

Similar overall behavior has been observed in samples of the other HVPE platelets, VPE2-331, and VPE2-155, the ODEPR immediately after irradiation showing only the negative L5 and EM signals, and the PL and ODEPR following roughly similar annealing behavior. In addition, in one more heavily irradiated VPE2-155 sample, the emergence of a weak L4 signal could be detected after room-temperature annealing. (The emergence of the correspondingly expected concentration of L3 could not be established due to its overlap with other existing spectra.) This appears to confirm that all of the spectra previously observed after room-temperature irradiation[9] are indeed produced in the room-temperature anneal of the low-temperature-irradiated samples, but not necessarily in the same relative concentrations. In these other samples, however, one significant difference is observed. The conversion of L5 to L6 is substantially greater than that shown for VPE2-180 in Fig. 3. This important difference, and a detailed study of the L5 to L6 conversion process, will be the subject of B, the accompanying paper immediately following this one.[11]

In the *p*-type MOVPE sample, the luminescence behavior is similar, the visible blue luminescence characteristic of *p*-type GaN decreasing with electron fluence at 4.2 K, and with the growth in of what appears to be the same broad 0.95-eV band in the IR. However, as reported earlier in a *p*-type sample from a different source,[18] heavier irradiation doses ($\sim 5\times$) are required. Some of the signals reported in the earlier *p*-type studies were also observed in the present sample, but not the $S=1$ center, labeled L8, that emerged in that work in the visible PL upon anneal at 180 K. Instead, the weak positive signal associated with interstitial Ga shown in Fig. 4(d) is observed to emerge in the IR after an anneal at 260 K, again also with the simultaneous emergence of a signal similar to that of L1. It disappears upon annealing at 300 K over a period of a few hours. Its estimated spin-Hamiltonian parameters are also included in Table I, where we have tentatively labeled it L6* because the deviation of its parameters from those for L6 is probably within the error of measurement for each. We recognize, however, that it could conceivably represent yet another slightly different Ga interstitial configuration. Its intensity was too weak to perform a detailed spectral dependence for it, but with selective filters it appears to originate from a slightly higher-energy portion of the 0.95-eV band, as opposed to L5 and L6 in the *n*-type HVPE materials, whose spectral dependences accurately mirror the complete band.

A careful study of the L1 signal in a separate 35-GHz ODEPR spectrometer after room-temperature anneal has revealed partially resolved structure[19] not noted in our initial study.[9] As shown in Fig. 6, it is greatly enhanced by second-derivative processing, and can be matched very well as the result of hyperfine interaction with three equivalent Ga atoms. [Here the sticks represent the relative intensity and positions for the lines arising from three identical $I=3/2$ Ga atoms, each with the normal abundance of their two stable isotopes, and with $A(^{69}\mathrm{Ga}) = 100$ MHz.] The hyperfine interaction appears isotropic with no distinguishable difference (± 10 MHz) between $\mathbf{B}\|\mathbf{c}$, and $\mathbf{B}\perp\mathbf{c}$. Resolution of the structure is, however, observed to depend somewhat upon orientation for **B** in the *c* plane, as is evident in the study in the 20-GHz ODEPR spectrometer shown in Fig. 7. Attempts to use the existence of this structure to establish whether or not L1*, the weak L1-like signal appearing to emerge at lower temperatures with L6, is identical to L1 have so far not been successful. The structure is not clearly evident in L1*

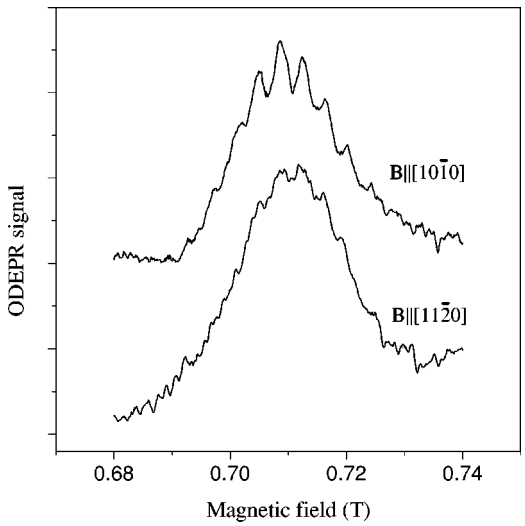

FIG. 7. Resolution of the L1 structure at two different orientations of **B** in the *c* plane.

but its weak intensity plus the uncertainty of the *c*-plane orientation in mounting the tiny samples for the *in situ* irradiation experiments make this observation so far inconclusive.

IV. DISCUSSION

A. ODEPR spectra

1. L5

The simultaneous 1:1 presence immediately after 4.2 K irradiation, and vs annealing, of the shallow effective-mass donor and the L5 resonances, both negative, reveals that the two signals result from a spin-dependent transfer process between the shallow donor and the deep L5 center, which is *competing* with, but not directly related to, the recombination process giving rise to the PL being observed. That the L5 center is deep, with the spin wave function highly localized, is evident from its hyperfine parameters in Table I. Comparing the values for $|A_{\|}|=a+2b$, and $|A_{\perp}|=a-b$ to Hartree-Fock estimates for the ^{69}Ga neutral free atom ($a=7430.4$ MHz for the $4s$, and $b=148.2$ MHz for the $4p$ orbital) (Ref. 20) gives, in a simple linear combination of atomic orbitals (LCAO) treatment, 52% of the spin wave function located in the $4s$ orbital and $\approx 54(\pm 8)\%$ in the $4p$ orbital of the Ga atom. (The indicated accuracy for the $4p$ contribution is the result of the probable error estimates in Table I and their significant effect in extracting the small anisotropy in the hyperfine parameters.) This simple calculation implies that $\approx 100\%$ of the wave function is accounted for on the Ga atom. It would be more appropriate, of course, to compare to the values for the Ga^{++} free ion, which are not directly available. However, a rough estimate can be made by scaling the neutral atom Hartree-Fock values by the ratio calculated for the isoelectronic $Al^{++}3s$ to $Al^{0}3s$ values,[20] ≈ 1.45. If we do that, the approximate 50-50 distribution between the $4s$ and $4p$ orbitals remains the same [36% $4s$, $37(\pm 6)\%$ $4p$] but the localization on the Ga atom becomes the more realistic $\approx 73(\pm 6)\%$, again highly localized.

The presence of L5 immediately after a 4.2 K irradiation clearly reveals it to be directly related to one of the intrinsic defects produced by the primary knock-on damage event. Two possibilities suggest themselves—the Ga interstitial in its Ga_i^0 or Ga_i^{2+} paramagnetic state, or a paramagnetic charge state of the nitrogen vacancy with the wave function highly localized on one of its four Ga neighbors, the result of a Jahn-Teller distortion. We can reasonably rule out the V_N^0 paramagnetic state because all theoretical calculations appear to agree that it should be a shallow effective-mass state.[2,3,6,7] The paramagnetic V_N^{2+} state can also be ruled out since it is not predicted by theory to exist in the bandgap,[3,6,7] and, even if it did exist,[2] it should be undistorted, with one electron in an orbitally nondegenerate a_1 state. Of the two Ga interstitial charge states, Ga_i^0 can also be reasonably ruled out because theory predicts it to be only a shallow EM state in either of its two possible sites (O or T),[6] but also because spin-dependent electron capture would carry it to a negative charge state, additionally unreasonable.

We conclude therefore that L5 must result from the Ga interstitial in its Ga_i^{2+} paramagnetic state, with its ODEPR detection along with that of EM^0 resulting from the spin-dependent process

$$Ga_i^{2+} + EM^0 \rightarrow Ga_i^{+} + EM^{+}. \quad (2)$$

Its disappearance upon extended anneal at room temperature with the simultaneous emergence of signals previously observed in earlier room-temperature irradiations, (including L4, which was previously suggested to be a trapped Ga interstitial), reveals, in addition, the important information that it executes sufficient long-range migration in the lattice at this temperature to be trapped by impurities or other defects.

2. L6

L6 clearly also originates from Ga_i^{2+}, with only slightly different spin-Hamiltonian parameters from those of L5. But its signal is *positive*, revealing a spin-dependent process that is directly or indirectly involved in the *production* of the 0.95-eV luminescence. A corresponding positive EM signal is not observed that correlates with it. Instead, the positive signal L1* appears to emerge in close correlation with L6. This suggests spin-dependent recombination between Ga_i^{2+} and the defect giving rise to L1*. Like L5, the L6 defect is also deep, with its spin wave function highly localized on the Ga atom. LCAO analysis similar to that for L5 using the Ga^{++} estimates gives it to be 37% localized in the $4s$ and $31(\pm 18)\%$ in the $4p$ orbital of the Ga^{2+} atom, with $\approx 68(\pm 18)\%$ localized on the atom. The character of the Ga_i^{2+} spin wave function for L6 is therefore very close to that for L5.

L6 must result from a different configuration for Ga_i^{2+} in the lattice than that for L5. This, therefore, implies motion of some kind for the interstitial even at 60 K, where, as shown in Fig. 3, it first appears in the *n*-type material, particularly in

the presence of optical illumination. The details of the L5 $\rightarrow$L6 conversion, and the role of optical excitation, will be presented in paper B. Here we note only that it is occurring, and that it implies motion of some kind for the interstitial.

*3. L6**

Like L6 in the *n*-type material, L6*, observed in *p*-type material, is also detected as a positive ODEPR signal and appears to be accompanied by a second positive signal indistinguishable from that of L1. Its spin-Hamiltonian parameters given in Table I are close enough to those of L6 to be the same within our experimental accuracy. It too is clearly associated with Ga_i^{2+}, but whether it arises from the identical configuration as L6, or reflects a third slightly different one, as perhaps suggested by its slightly different PL spectral dependence, cannot be determined at this stage. We will not consider it further in the present paper, a more comprehensive study in *p*-type materials being required to resolve this question.

4. L1

The L1 signal can be produced in *n*-type material both by room-temperature irradiation, and by annealing at room temperature after low-temperature irradiation. In these materials, it can always be observed in the irradiation-produced 0.95-eV band under UV excitation (3.53 or 3.41 eV) and it disappears when the band disappears upon annealing at $\sim$500 °C.[9] On the other hand, L1 is not observed for argon-ion excitation energies of 2.73 eV or below, even though the PL band is present for excitation energies down to and including the 1.52-eV line. L1 is therefore directly involved in a spin-dependent feeding process for the 0.95-eV PL but this process is not *the* luminescence process itself.[9]

The resolved nearly isotropic hyperfine interaction with three Ga atoms of $a=100$ MHz, amounts, when compared to the neutral Ga free atom values, to only $\sim$1.4% 4*s* character on each, or a total of only $\sim$4%. Setting an upper limit for the possible undetected hyperfine anisotropy of $3b \leqslant 15$ MHz, as given by the experimental uncertainty, ± 10 MHz, gives $\leqslant$3.5% 4*p* on each, for a total of somewhere between 4 and 15% of the wave function distributed between the three. The wave function is therefore not highly localized on these three Ga atoms.

Three models possibly consistent with the Ga hyperfine interactions have been suggested.[19]

a. Trapped nitrogen vacancy. Here one of the four neighboring Ga atoms is replaced by an impurity. Since the nitrogen vacancy is believed to be a shallow donor, a logical impurity might be a Group-II atom such as Mg or Zn, each of which is an acceptor. Each has only a low-abundance nuclear-spin isotope, leaving the three remaining Ga near neighbors to the vacancy to produce the hyperfine structure.

b. Trapped Ga vacancy. Here one of the four *N* neighbors is replaced by an impurity. Since the Ga vacancy is a deep acceptor, a logical impurity trap would be a substitutional Group-VI donor, such as O or S, which also have low-abundance nuclear-spin isotopes. In this case, the relatively weak hyperfine interactions could come from the three Ga atoms back bonded to the impurity. In this model, the dominance of the Ga hyperfine interactions over those of the three near-neighbor N atoms would be helped by the $\sim$5 times greater Ga atomic hyperfine values over those for atomic N. The N interactions could provide the remaining broadening.

c. Isolated Ga vacancy. In cubic GaN, a Jahn-Teller distortion would be expected for the V_{Ga}^{2-} paramagnetic charged state because it has one hole (t_2^5) in a degenerate t_2 orbital.[21] In analogy to its isoelectronic t_2^5 counterpart V_{Zn}^{-} in ZnSe, one of its four neighbors would distort inward, and the hole would tend to localize on that neighbor.[22] In wurtzite GaN, where the local departure from cubic symmetry corresponds to compression along the *c* axis, this means that the localization will tend to be onto the on-axis nitrogen neighbor. In this model, therefore, the unpaired spin wave function is shifted toward the on-axis N and its three back-bonded Ga atoms. Again, as for the trapped vacancy, these Ga atoms would account for the resolved structure, and the nitrogen hyperfine interactions would have to be weak enough to serve primarily to broaden the lines. (We note briefly also the interesting prediction of Chadi that a N neighbor could move into the vacant Ga site to produce what is in effect a N antisite next to a N vacancy, which would be a triple donor and 3.2 eV more stable when the Fermi level is at the valence-band edge.[23] The N vacancy produced by this transformation would have three Ga neighbors, suggesting another interesting possibility for the three-Ga hyperfine interactions, as for the trapped nitrogen vacancy considered above. However, this transformation is predicted to occur only in strongly *p*-type material, the 3.2-eV energy difference having vanished already when the Fermi level has risen by only $\sim$0.6 eV. Therefore, in our case of *n*-type material, it should not be a consideration.)

Model (a) requires the motion at room temperature of the N vacancy, and model (b) that of the Ga vacancy. Of course, either is possible, and we cannot rule them out. However, the onset of long-range migration for either almost simultaneously with that of the Ga interstitial would be a coincidence. On the other hand, the emergence of the isolated Ga vacancy could follow naturally as its perturbing nearby Ga interstitial migrates away.

B. 0.95-eV photoluminescence

The 0.95-eV PL is present immediately after the 4.2 K irradiation. It, therefore, must arise from an intrinsic defect itself. Although $\sim$85% of it is lost after room-temperature annealing, the remaining component, which is indistinguishable in spectral shape from that immediately after irradiation, is stable to $\sim$500 °C. This suggests that it is associated with an intrinsic defect that is stable up to $\sim$500 °C, but for which the PL intensity drops dramatically when the Ga interstitial begins to migrate and become trapped.

V. MODEL

In Fig. 8, we first present a simple schematic model which summarizes what our results appear to suggest concerning the origin of the 0.95-eV luminescence and the ODEPR sig-

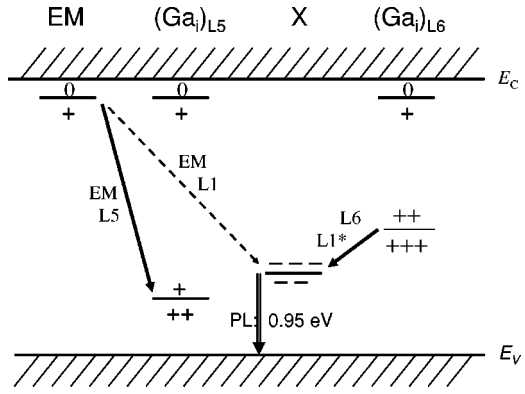

FIG. 8. Schematic model for the origin of the PL and ODEPR signals.

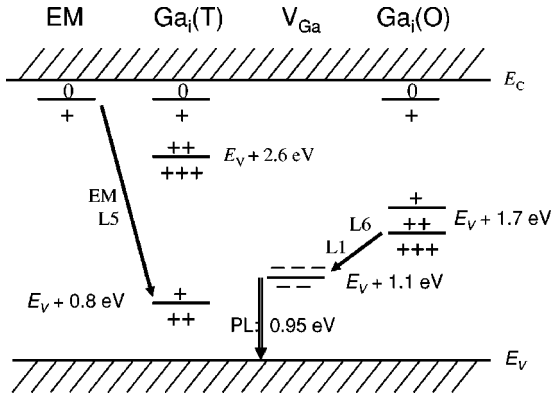

FIG. 9. Model I, identifying L5 and L6 with Ga_i^{2+} in the *T* and *O* interstitial sites, respectively, and L1 with the Ga vacancy (V_{Ga}^{2-}). The indicated level positions for the interstitials come from Ref. 6, the value for V_{Ga} from Ref. 5.

nals. Here, the 0.95-eV luminescence is the result of hole capture from the valence band by a radiation-produced defect which we label *X*. The exact configurations for the two interstitials are not specified so they are labeled simply $(Ga_i)_{L5}$ and $(Ga_i)_{L6}$. As shown, the electrical level position of $(Ga_i^{2+})_{L6}$ is placed above the level for *X*, so that transfer of an electron from it to *X* can occur, feeding the luminescence and producing the positive L6 + L1* resonances. Electron transfer from the shallow EM state to $(Ga_i^{2+})_{L5}$, whose electrical level position is placed below that for *X*, is in competition with processes feeding the luminescence because the electron cannot subsequently be transferred to *X*. The EM and L5 signals are therefore negative. Shown also as a dashed line is a less efficient direct electron transfer from the shallow EM donor to *X*, which emerges as positive EM and L1 signals only after annealing at room temperature. In this model the L1* and L1 resonances are identical, coming from the same electron-receiving state of *X*.

Further progress beyond this requires the construction of reasonable models for the specific interstitial configurations involved, as well as for the defect *X* that is responsible for the 0.95-eV PL. We now present two such models.

A. Model I

In Fig. 9, we show that the schematic model of Fig. 8 can be fit very nicely with recent calculations for the electrical level positions if we identify L5 with Ga_i^{2+} in the interstitial *T* site, L6 with Ga_i^{2+} in the interstitial *O* site, and L1, which arises from the *X* defect, with a nearby Ga vacancy in its paramagnetic V_{Ga}^{2-} state. As shown, in the *T* site, $Ga_i(T)$ has been predicted to be a triple donor, with its second and third donor states deep and in strongly negative-*U* ordering, the relevant second donor level $(+/++)$ being at $E_V + 0.8$ eV,[6] where E_V denotes the energy at the top of the valence band. For $Ga_i(O)$ at the *O* site, the second and third donor levels are predicted to be very close in energy, centered around $E_V + 1.7$ eV,[6] or in negative-*U* ordering at $E_V + 1.9$ eV (Ref. 3) or $E_V + 2.25$ eV.[4] For each configuration, the first donor level is predicted to be shallow and EM-like. For the triple acceptor level of V_{Ga} $(3-/2-)$, its position has been predicted to be at $E_V + 1.1$ eV.[5]

This model, therefore, fits remarkably well, locating all of the relevant energy levels where they have to be to explain the ODEPR signals. In particular also, the V_{Ga} level prediction at $E_V + 1.1$ eV is remarkably close to what is required to account for the broad Stokes-shifted PL band centered at 0.95 eV. In addition, the identification of the 0.95-eV luminescing center (*X*) as the gallium vacancy satisfies the further requirement that it be identified with an intrinsic defect. We have already presented arguments for the possible identification of its L1 signal with V_{Ga}^{2-}. In this model, the luminescence results when nonparamagnetic V_{Ga}^{3-} captures a hole, the ODEPR signals arising from competing and/or feeding processes that vie for the required electron transfer to its paramagnetic V_{Ga}^{2-} state, and not the luminescence process itself, as required. As initially produced, each Ga vacancy has a positively charged Ga interstitial nearby, and the electron feeding processes to the negatively charged vacancy should therefore be strongly favored to go by way of the Coulomb-attractive interstitial. When the Ga interstitials start to migrate at room temperature, presumably some recombine with the vacancies, others get away and become trapped. At this point, the remaining isolated Ga vacancies can be fed by a less efficient process directly from the shallow donors, producing the L1 ODEPR signal. This model therefore serves to explain the ODEPR and PL changes during annealing at room temperature in terms of one mobile species—the interstitial. In this model, the low-temperature conversion between L5 and L6 is the result of interchange of the interstitial between its *T* and *O* sites. This motion constitutes a half diffusion step, implying migrational motion of some kind for the interstitial also at this low temperature.

Although this model is very attractive in that it appears to explain essentially everything that has been observed, there is a serious concern that must be addressed. It requires Ga_i^{2+} to have almost identical hyperfine interactions in the *T* and *O* sites (within $\sim 2-3\%$). Is that reasonable? Maybe, but let us consider an alternative model.

B. Model II

In Fig. 10 we consider a very similar model, but with the exception that the two different Ga_i^{2+} sites are each *T* sites,

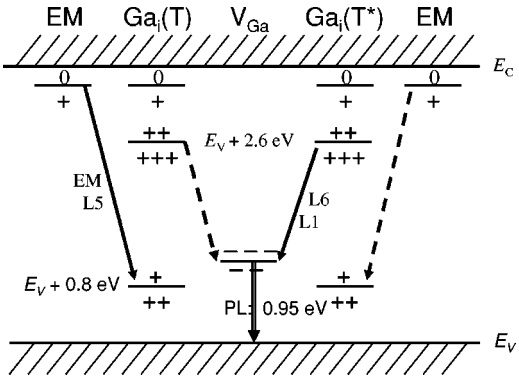

FIG. 10. Model II, identifying L5 and L6 as arising from $Ga_i^{2+}(T)$ and $Ga_i^{2+}(T^*)$, respectively, both in T sites, but with T^* closer to its V_{Ga}. As in Model I, L1 and the 0.95-eV PL are identified with the Ga vacancy (V_{Ga}). The solid lines represent the dominant transitions.

with, therefore, very similar hyperfine interactions. We retain the identity of V_{Ga} with the 0.95-eV PL and with the L1 ODEPR, but look more closely at the level positions predicted by theory for $Ga_i(T)$. A third donor level ($++/+++$) is actually predicted to be at $E_V+2.6$ eV, as shown in the figure, and the spin-dependent *feeding* process, which we did not consider in Model I,

$$Ga_i^{2+}(T)+V_{Ga}^{2-}\rightarrow Ga_i^{3+}(T)+V_{Ga}^{3-} \tag{3}$$

could also occur from each T site as well, in addition to the spin-dependent competitive process of Eq. (2). On the left side of Fig. 10, we consider the Ga_i to be several lattice sites removed from the V_{Ga} from which it was ejected, a logical assumption for the average distance after a 2.5-MeV irradiation displacement event. In that case, since both Ga_i^{2+} and V_{Ga}^{2-} are deep, with highly localized wave functions, their electronic overlap is weak, and transfer in the *n*-type material from the large orbit shallow EM donors to Ga_i^{2+}, Eq. (2), dominates, producing the negative EM and L5 ODEPR signals.

For $Ga_i^{2+}(T^*)$, where T^* is a T site closer to V_{Ga}^{2-}, the enhanced overlap of their wave functions could now make the electron-transfer process between them, Eq. (3), become dominant, as shown on the right-hand side of Fig. 10, giving rise to the dominance of the positive signals L6 and L1. The presence of the closer V_{Ga}^{2-} would account for the slightly different hyperfine interaction for L5 and L6. (The fact that there appears to be a single unique L6 suggests a particularly stable near-neighbor position, such as, for example, with a nearest neighbor N atom separating it from the vacancy, in analogy to the observation in the annealing for Zn_i in ZnSe.[24])

Here, the low-temperature conversion between L5 and L6 involves motion between two T sites, in this case a full diffusion step, implying again motion of some kind for the interstitial at this low temperature.

VI. SUMMARY

We have established the following: Interstitial Ga_i^{2+} has been observed in two different configurations by ODEPR in undoped *n*-type GaN after *in situ* 2.5-MeV electron irradiation at 4.2 K. In one, signal L5, it is observed via a spin-dependent process involving electron transfer from the shallow EM donor to it, which is competing with spin-independent processes feeding an irradiation-produced 0.95-eV luminescence band. In the other, signal L6, it is observed via a spin-dependent process of electron transfer between it and a defect giving rise to signal L1*, which is feeding the luminescence. Only L5 is observed immediately after irradiation, but conversion between the two configurations can occur at as low a temperature as 60 K, and aided by optical excitation. Long-range migration, with subsequent trapping of the interstitial, occurs over a period of several hours at room temperature. Within experimental accuracy, L1* has the same g values and width as L1, the signal that grows in upon annealing at room temperature and which is stable to $\sim 500\,^{\circ}$C, where the irradiation-produced 0.95-eV luminescence also disappears. Having been created by irradiation *in situ* at 4.2 K, the 0.95-eV band must also arise from an intrinsic defect.

Two tentative Ga_i-V_{Ga} Frenkel-pair models have been presented to explain the results. One identifies L5 as arising from Ga_i^{2+} in a nearby T interstitial site of the wurtzite lattice, and L6 as arising from Ga_i^{2+} in a nearby O site. The other identifies L5 and L6 as arising from Ga_i^{2+} in two different nearby T sites, with L6 arising from Ga_i^{2+} in a site that is closer to its V_{Ga} partner. In each model, the T site has been chosen to play a role because it easily provides a simple mechanism for the competing process involving L5. This is fully consistent with the calculations of Boguslawski *et al.*,[6] which predict the T site to be ~ 0.2 eV more stable than the O site. We note, however, that the calculations of Neugebauer and Van de Walle[4] predict the T site to be less stable than the O site, by ~ 1 eV. This provides another reason to consider these models tentative, although in the low-temperature radiation damage production process, the exact configurations that result do not necessarily reflect the thermodynamically stable ones. In each of these models, conversion between L5 and L6 implies that diffusional motion of some kind can occur for the interstitial Ga atoms at cryogenic temperatures. Thermally activated long-range migration of the interstitial, on the other hand, appears not to occur until annealing at room temperature. This strongly suggests that the cryogenic temperature motion must be associated with the optical excitation. This will be explored in more detail in B, the accompanying paper that follows.[11]

The 0.95-eV luminescence is proposed to arise from hole capture by the triply negatively charged Ga vacancy V_{Ga}^{3-} and with the identical L1 and L1* ODEPR signals arising from its V_{Ga}^{2-} paramagnetic state. If this is correct, the stability of the 0.95-eV PL and the L1 ODEPR signal to 500 °C provides the important additional information that the isolated gallium vacancy is stable to this temperature.

Finally, the correct interpretation of our results would be greatly assisted by further calculations on several specific

points concerning the defects involved, and we would like to take this opportunity to encourage theorists to tackle them. They include: (1) estimation of the central hyperfine interaction for interstitial Ga in the *T* and *O* sites; (2) determination of the spin wave function for V_{Ga}^{2-} to test whether its distribution among the neighbors is consistent with its identification as L1; and (3) further resolution of the question of the relative stability of the two Ga interstitial sites *T* and *O*.

Note added in proof. Van de Walle informs us that further calculations[25] confirm the ~1 eV higher energy for the *T* site and, in addition, find it a saddle-point configuration and therefore not even a local metastable minimum. Assuming this to be correct, our models, both of which involve the *T* site, must be reconsidered. One likely alternative is that the two sites in model II are *O* sites, again distant from (giving L5) and close to (giving L6) the Ga vacancy.

ACKNOWLEDGMENTS

This research was supported jointly by Office of Naval Research Grant No. N00014-94-1-0117 and National Science Foundation Grants Nos. DMR-97-04486 and DMR-00-93784.

*Present address: Department of Physics, University of Alberta, Edmonton, AB, Canada T6G 2J1.
†Present address: A. F. Ioffe Physico-Technical Institute, 194201 St. Petersburg, Russia.
‡Present address: Danfoss A/S, DK-6430 Nordborg, Denmark.
§Present address: Nova Measuring Instruments Inc., 3080 Olcott St., Suite 210B, Santa Clara, CA 95094.
¶Present address: Furukawa Co. Ltd., Kannondai 1-25-13, Tsukuba, Ibaraki 305-0856 Japan.

[1] For a recent review, see H. Morkoç, Mater. Sci. Forum **239–241**, 119 (1997).
[2] D.W. Jenkins, J.D. Dow, and Min-Hsiung Tsai, J. Appl. Phys. **72**, 4130 (1992).
[3] J. Neugebauer and C.G. Van de Walle, Phys. Rev. B **50**, 8067 (1994).
[4] J. Neugebauer and C.G. Van de Walle, in *Festkörperprobleme/ Advances in Solid State Physics*, edited by R. Helbig (Viewig, Braunschweig/Wiesbaden, 1996), Vol. 35, p. 25.
[5] J. Neugebauer and C.G. Van de Walle, Appl. Phys. Lett. **69**, 503 (1996).
[6] P. Boguslawski, E.L. Briggs, and J. Bernholc, Phys. Rev. B **51**, 17 255 (1995).
[7] I. Gorczyca, A. Svane, and N.E. Christensen, Phys. Rev. B **60**, 8147 (1999).
[8] M. Linde, S.J. Uftring, G.D. Watkins, V. Härle, and F. Scholz, Phys. Rev. B **55**, R10 177 (1997).
[9] C. Bozdog, H. Przybylinska, G.D. Watkins, V. Härle, F. Scholz, M. Mayer, M. Kamp, R.J. Molnar, A.E. Wickenden, D.D. Koleske, and R.L. Henry, Phys. Rev. B **59**, 12 479 (1999).
[10] K.H. Chow, G.D. Watkins, Akira Usui, and M. Mizuta, Phys. Rev. Lett. **85**, 2761 (2000).
[11] P. Johannesen, A. Zakrzweski, L.S. Vlasenko, G.D. Watkins, Akira Usui, Haruo Sunakawa, and Masashi Mizuta, following paper, Phys. Rev. B **69**, 045208 (2004).
[12] A. Usui, H. Sunakawa, A. Sakai, and A.A. Yamaguchi, Jpn. J. Appl. Phys. **36**, L899 (1997).
[13] F.C. Rong, W.A. Barry, J.F. Donegan, and G.D. Watkins, Phys. Rev. B **54**, 7779 (1996).
[14] C. Bozdog, G.D. Watkins, H. Sunakawa, N. Kuroda, and A. Usui, Phys. Rev. B **65**, 125207 (2002).
[15] E.R. Glaser, J.A. Freitas, Jr., G.C. Braga, W.E. Carlos, M.E. Twigg, A.E. Wickenden, D.D. Koleski, R.L. Henry, M. Leszczynski, I. Grzegory, T. Suski, S. Porowski, S.S. Park, K.Y. Lee, and R.J. Molnar, Physica B **308-310**, 51 (2001).
[16] J. Baur, U. Kaufmann, M. Kunzer, J. Schneider, H. Amano, I. Akasaki, T. Detchprohm, and K. Hiramatsu, Mater. Sci. Forum **196–201**, 55 (1995).
[17] W.E. Carlos, J.A. Freitas, Jr., M. Asif Khan, D.T. Olson, and J.N. Kuznia, Phys. Rev. B **48**, 17 878 (1993).
[18] L.S. Vlasenko, C. Bozdog, G.D. Watkins, F. Shahedipour, and B.W. Wessels, Phys. Rev. B **65**, 205202 (2002).
[19] G.D. Watkins, L.S. Vlasenko, and C. Bozdog, Physica B **308–310**, 62 (2001).
[20] A.K. Koh and D.J. Miller, At. Data Nucl. Data Tables **33**, 235 (1985).
[21] G.D. Watkins, in *Handbook of Semiconductor Technology*, edited by K.A. Jackson and W. Schroter (Wiley-VCH, Weinheim, 2000), Vol. 1, Chap. 3.
[22] G.D. Watkins, J. Cryst. Growth **159**, 338 (1996).
[23] D.J. Chadi, Appl. Phys. Lett. **71**, 2970 (1997).
[24] G.D. Watkins, Phys. Rev. Lett. **33**, 223 (1974).
[25] S. Lompijumnong and C.G. Van de Walle, Phys. Rev. B **69**, 035207 (2004).